THE JOURNAL OF PHYSICAL CHEMISTRY B

Article

pubs.acs.org/JPCB

Fluorescence Quenching of (Dimethylamino)naphthalene Dyes Badan and Prodan by Tryptophan in Cytochromes P450 and Micelles

Petr Pospíšil,[†] Katja E. Luxem,[‡] Maraia Ener,[‡] Jan Sýkora,[†] Jana Kocábová,[†] Harry B. Gray,*[,‡] Antonín Vlček, Jr.,*[,†,§] and Martin Hof*[,†]

[†]J. Heyrovský Institute of Physical Chemistry, Academy of Sciences of the Czech Republic, Dolejškova 3, CZ-182 23 Prague, Czech Republic

[‡]Beckman Institute, California Institute of Technology, Pasadena, California 91125, United States

[§]School of Biological and Chemical Sciences, Queen Mary University of London, Mile End Road, London E1 4NS, United Kingdom

Supporting Information

ABSTRACT: Fluorescence of 2-(*N*,*N*-dimethylamino)-6-propionylnaphthalene dyes Badan and Prodan is quenched by tryptophan in Brij 58 micelles as well as in two cytochrome P450 proteins (CYP102, CYP119) with Badan covalently attached to a cysteine residue. Formation of nonemissive complexes between a dye molecule and tryptophan accounts for about 76% of the fluorescence intensity quenching in micelles, the rest is due to diffusive encounters. In the absence of tryptophan, fluorescence of Badan-labeled cytochromes decays with triexponential kinetics characterized by lifetimes of about 100 ps, 700−800 ps, and 3 ns. Site mutation of a histidine residue in the vicinity of the Badan label by tryptophan results in shortening of all three decay lifetimes. The relative amplitude of the fastest component increases at the expense of the two slower ones. The average quenching rate constants are 4.5×10^8 s^{-1} (CYP102) and 3.7×10^8 s^{-1} (CYP119), at 288 K. Cyclic voltammetry of Prodan in MeCN shows a reversible reduction peak at −1.85 V vs NHE that becomes chemically irreversible and shifts positively upon addition of water. A quasireversible reduction at −0.88 V was observed in an aqueous buffer (pH 7.3). The excited-state reduction potential of Prodan (and Badan) is estimated to vary from about +0.6 V (vs NHE) in polar aprotic media (MeCN) to approximately +1.6 V in water. Tryptophan quenching of Badan/Prodan fluorescence in CYPs and Brij 58 micelles is exergonic by ≤0.5 V and involves tryptophan oxidation by excited Badan/Prodan, coupled with a fast reaction between the reduced dye and water. Photoreduction is a new quenching mechanism for 2-(*N*,*N*-dimethylamino)-6-propionylnaphthalene dyes that are often used as solvatochromic polarity probes, FRET donors and acceptors, as well as reporters of solvation dynamics.

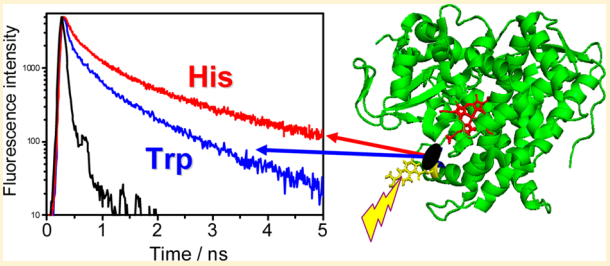

INTRODUCTION

Fluorescence quenching of organic dyes appended to proteins occurs either by energy transfer (FRET) or, less often, by electron transfer (ET).[1,2] Quenching kinetics provide important information on substrate binding, conformational changes, intraprotein interactions, and protein folding, among others.[1−7] FRET rates fall with the sixth power of the donor−acceptor distance and can be used to map relatively long-range interactions, from about 1 to 10 nm. On the other hand, the exponential decay of ET rates with distance[8] allows investigating shorter-range interactions around 1 nm and below. Given the short inherent excited-state lifetimes of organic chromophores (typically 2−8 ns), only very fast ET leads to efficient fluorescence quenching. This usually happens only when the electron donor and acceptor come into a close contact, for example, by $\pi\pi$ stacking and/or hydrophobic forces.[3,4,9] Such interactions are then manifested by static fluorescence intensity quenching whereas fluorescence decay becomes multiexponential, showing very fast (usually tens of picosecond or less) kinetics component(s) due to emission from donor−acceptor contact complexes, and an unquenched decay due to residual free fluorophore.[1,2] The on−off ET fluorescence switching upon emergence of a close donor−acceptor contact also can be detected by single-molecule techniques, such as fluorescence correlation spectroscopy, showing intensity fluctuations that report on protein conformational changes, folding, or on interaction dynamics, with applications in biomolecular recognition and molecular diagnostics.[3,4,10,11] Fluorescence ET quenching in proteins has been studied mainly using oxazine, rhodamine, or Bodipy dye labels as excited-state electron acceptors (oxidants) and tryptophan (Trp) indole side chains as electron donors.[3,4,10,11] Fluorescence of a variety of dyes also can be quenched by ET from a thioamide group incorporated into the peptide backbone, as has been employed to investigate protease activity and protein folding.[12] Notably, electronically excited flavodox-

Received: May 11, 2014
Revised: July 7, 2014
Published: July 31, 2014

   dx.doi.org/10.1021/jp504625d | J. Phys. Chem. B 2014, 118, 10085−10091

ine cofactors are quenched by ET from Trp in photolyases and cryptochromes, which are involved in DNA photorepair and blue-light sensing by living organisms, respectively.[13−16]

We have investigated fluorescence quenching of two 2-(*N*,*N*-dimethylamino)-6-propionylnaphthalene dyes Badan and Prodan to Trp in two cytochrome P450 mutants and in Brij 58 micelles (Figures 1 and 2). Fluorescence of dimethylnaphthalene-based dyes originates from an intramolecular charge-transfer excited state in which electron density is transferred from the NMe_2 group to the electron-accepting carbonyl substituent at the naphthalene 6-position.[1,2,17−19] These photophysics are strongly medium-dependent, presumably due to the molecular dipole moment increasing upon excitation and specific solvation, including hydrogen bonding.[2,19] The dyes are frequently used as probes of polarity and dynamics of the local environment in proteins[1,20,21] as well as micelles and membranes,[1,2,17,18] by measuring stationary and time-resolved fluorescence spectra.[1] The environmental dependence of Badan fluorescence lifetimes was employed, for example, in a glucose sensor.[22] These utilities prompted the development of dimethylnaphthalene-based dyes with a broad range of protein labeling groups, including Badan (thiol-reactive bromine, Figure 1), Acrylodan (cysteine-reactive ethylene), the unnatural amino acid Aladan for incorporation into peptide chains, Danca, which binds apomyoglobin in a single orientation through a carbonycyclohexyl group, and Dansyl, where the 6-propionyl is replaced by a sulfonamide. Prodan (and its derivatives with long aliphatic chains) are typically used as noncovalent membrane probes.[1,17]

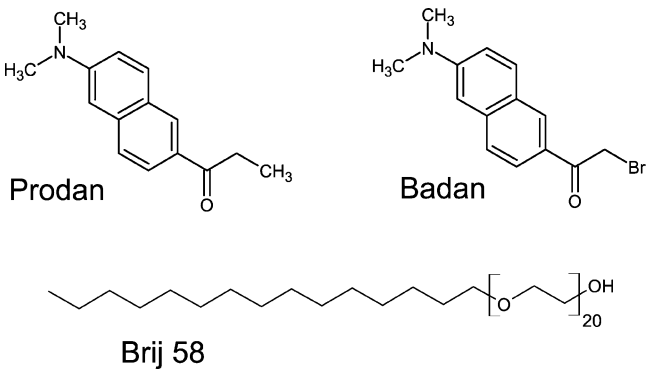

Figure 1. Prodan and Badan dye molecules (top) and the Brij 58 detergent molecule.

(Dimethylamino)naphthalene-type dyes also serve as energy acceptors from electronically excited tryptophan, *Trp,[1,23] or as energy donors toward hemes in cytochromes,[24,25] as utilized in FRET experiments. Photoinduced electron transfer, in contrast, is not a common quenching mechanism of these dyes, although Badan photoreduction by Trp was proposed to occur in one of the CYP3A4 conformers.[5] An opposite process, photooxidation of a (dimethylamino)naphthalene by a guanine cation, has been observed in a protein−DNA complex.[26]

Herein, we present compelling evidence for ET quenching of Badan fluorescence by comparing the behaviors of Badan-labeled cytochrome P450 mutants (CYP, Figure 2) with and without a Trp residue in the dye vicinity. The occurrence of photoinduced ET from Trp to electronically excited 2-(dimethylamino)-6-propionylnaphthalene dyes is further supported by electrochemistry and by fluorescence quenching of Badan and Prodan in Trp-containing micelles. Observation of an ET quenching mechanism for these dyes highlights an important constraint for their use as microenvironmental probes, while opening new avenues for study of ultrafast dynamics associated with short-range interactions in biological systems.

EXPERIMENTAL SECTION

Materials. Badan and Prodan were obtained from Anaspec and Invitrogen, respectively, and used without further purification. Brij 58 and tryptophan were obtained from Sigma-Aldrich.

Protein Expression. The CYP102 (also called P450 BM3 or CYP102(A1)) C62A/C156S/K97C triple mutant has been

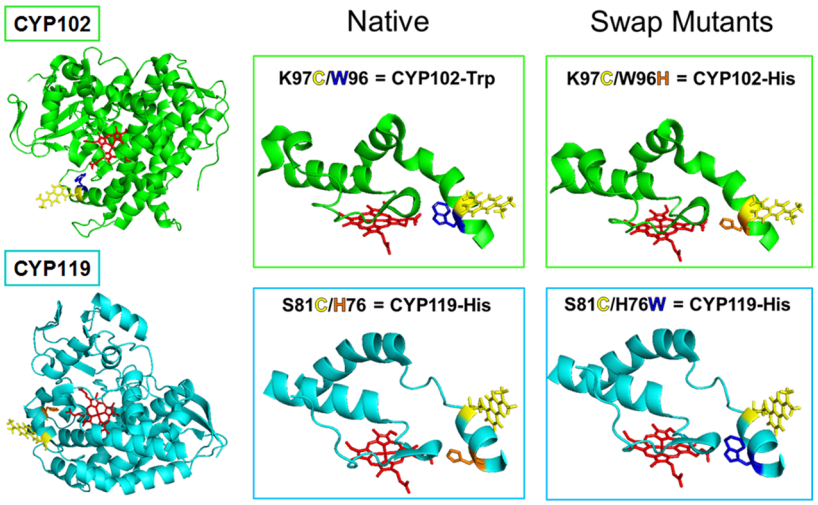

Figure 2. Schematic structures and abbreviations of the investigated Badan-labeled cytochrome P450 mutants *Bacillus megaterium* CYP102 (top, also known as P450 BM3 or CYP102(A1)) and *Sulfolobus acidocaldarius* CYP119 (bottom). Badan (yellow) is attached to Cys97 and Cys81, respectively. Native residues Trp96 of CYP102 and His76 of CYP119 (middle panels) are replaced by His96 and Trp76, respectively, in the swap mutants (right panels). The heme is shown in red, His in orange, Trp in blue, and Cys and Badan in yellow. Based on unlabeled protein structures: pdb 2IJ2[27] (CYP102-Trp), pdb 1IO7[28] (CYP119-His), and yet unpublished structure of CYP102-His. The Badan orientation was chosen arbitrarily for illustrative purposes.

dx.doi.org/10.1021/jp504625d | *J. Phys. Chem. B* 2014, 118, 10085−10091

reported.[29] The His-containing mutant C62A/C156S/K97C/W96H and CYP119 mutants S81C/H86 and S81C/H76W were prepared by the same procedure. The plasmid for CYP119 was obtained from Prof. Paul Ortiz de Montellano (UCSF). All mutations were made using a QuickChange Site-Directed Mutagenesis kit (Qiagen). All primers were obtained from Operon. The proteins were expressed with an N-terminal His_6 tag in *Escherichia coli* BL21(DE3) cells as described previously.[29] All proteins were purified according to a literature procedure[29] and characterized by ESI mass spectrometry.

Protein Labeling. Approximately a 5-fold molar excess of Badan was added to a 10 μM solution of protein in 20 mM Tris buffer (pH 8), and the mixture was shaken in the dark at 4 °C for 4 h. Excess Badan was removed during concentration in 30 kDa filters, and the protein was purified on a PD-10 desalting column (GE Healthcare and Life Sciences). Mass spectrometry indicated that the samples were labeled to 75−100%. Concentrated protein samples were stored with dithiothreitol (DTT, to prevent disulfide bond formation) in 25% glycerol solutions at −80 °C. Prior to use, they were thawed on ice and DTT was removed using a HiTrap desalting column (GE Healthcare Bio-Science AB, Uppsala) in a 20 mM Tris (pH 8) buffer. Samples were stored in the dark at 4 °C.

Preparation of Badan/Tryptophan-Containing Micelle Solutions. Badan (or Prodan) was added in a 1:2000 ratio to a ∼8 mM solution of the detergent Brij 58 in 20 mM Tris buffer (pH 8). The Brij 58 concentration was kept 2 orders of magnitude above the critical micelle concentration (CMC ∼ 0.08 mM).[30] Trp was dissolved separately in a basic aqueous solution (NaOH, pH ∼ 12). Aliquots of the Trp solution were added stepwise to the solution of Badan-containing micelles to achieve desired Trp concentrations. Samples were mixed by manually shaking directly in the cuvette, followed by measuring stationary fluorescence spectra and decay traces. To measure corresponding I_0 and τ_0 values, the same aliquots of aqueous NaOH solution not containing Trp were added to the same micelle/dye stock solution, eliminating thus possible pH and concentration effects on the quenching measurements. The Trp concentration range examined in Badan quenching experiments was limited to about 20 mM because Badan aggregation occurred at higher Trp concentrations due to increased pH. Aggregation onset was indicated by a fluorescence red shift and lifetime shortening.

Instrumentation. *Fluorescence.* Stationary emission spectra were obtained on a Fluorolog-3 spectrofluorometer (model FL3-11; HORIBA Jobin Yvon) equipped with a Xenon-arc lamp. All spectra were collected in 1 nm steps (2 nm bandwidths were chosen for both the excitation and emission monochromators). Time-resolved fluorescence decays were measured using the time-correlated single photon counting technique on an IBH 5000 U SPC instrument equipped with a cooled Hamamatsu R3809U-50 microchannel plate photomultiplier with 40 ps time resolution and time setting of 7 or 14 ps per channel. Bandwidths for both the excitation and emission monochromators were set to 16 nm. To eliminate scattered light, a 399 nm cutoff filter was used. Samples were excited at 373 nm with an IBH NanoLED-11 diode laser (80 ps fwhm) with a repetition frequency of 1 MHz. The detected signal was kept below 20 000 counts per second to avoid shortening of the recorded lifetime due to the pile-up effect. Fluorescence decays were fitted (using the iterative reconvolution procedure with IBH DAS6 software) to a multiexponential function (eq 1) convoluted with the experimental response function IRF ("prompt"), yielding sets of lifetimes τ_i and corresponding amplitudes A_i. The average lifetimes $\langle\tau\rangle$ were calculated according to eq 2.

$$I(t) = \sum_i A_i e^{-t/\tau_i} \otimes \mathrm{IRF} \tag{1}$$

$$\langle\tau\rangle = \frac{\sum_i A_i \tau_i^2}{\sum_i A_i \tau_i} \tag{2}$$

We also report relative lifetime-weighted amplitudes B_i that are proportional to the relative number of photons emitted in a kinetics component i (eq 3).

$$B_i = \frac{A_i \tau_i}{\sum_i A_i \tau_i} \times 100 \tag{3}$$

Electrochemistry. Cyclic voltammograms were obtained in MeCN containing 0.1 M Bu_4NPF_6 as an electrolyte and in aqueous Britton-Robinson buffer (pH = 7.3, I = 90 mM), using a home-built system for cyclic voltammetry consisting of a fast rise-time potentiostat, interfaced to a personal computer via an IEEE-interface card (AdvanTech, model PCL-848) and a data acquisition card (PCL-818) using 12-bit precision for A/D and D/A conversions. Electrochemical measurements were performed in a three-electrode electrochemical cell with a hanging Hg drop working electrode, a platinum mesh auxiliary electrode and Ag/AgCl/1 M LiCl reference electrode, which was separated from the test solution by a salt bridge with two frit junctions and whose potential (−90 mV vs NHE) was calibrated using the Fc^+/Fc couple as an internal standard (+0.54 V at a Pt working electrode vs Ag/AgCl/1 M LiCl; +0.630 V vs NHE[31]). All potentials are reported vs NHE.

RESULTS

Fluorescence Quenching in Badan-Labeled CYP Mutants. All four investigated CYPs show a typical Badan fluorescence band at about 485 nm using excitation at 373 nm (Figure S1, Supporting Information). Fluorescence decay was investigated at 550 nm, within the red side of the emission band. (The emission wavelength of 550 nm was chosen to avoid interference from fast decay components due to medium relaxation instead of population decay. These relaxation dynamics are currently under investigation in our laboratories.) Figure 3 shows that fluorescence decays of CYP102-Trp and CYP119-Trp were faster than in the case of their His counterparts.

Emission decay kinetics were multiexponential for all mutants, regardless whether Trp or His was present. Fitting to a triple exponential function yielded kinetics components occurring in the tens-of-picosecond (τ_1), hundreds-of-picosecond (τ_2), and nanosecond (τ_3) ranges (Table 1). Substituting His by Trp shortened all three lifetimes and strongly increased the relative amplitude of the fastest process, A_1 and B_1 indicating that the excited-state quenching reactions occur in several parallel pathways with lifetimes ranging from tens of picoseconds to tens of nanoseconds. The average quenching rate constants $\langle k_q\rangle$ (eq 4) are comparable for CYP119-Trp and CYP102-Trp (4×10^8 s^{-1} at 288 K), whereas the quenching rate constant $k_{q,3}$ (based on the slow kinetics component τ_3) is 1.4−1.6 times higher for CYP102-Trp, in accordance with a shorter Trp−Badan distance (Figure 2). As expected, both quenching rate constants slightly decreased on decreasing the temperature from 296 to 288 K.

dx.doi.org/10.1021/jp504625d | J. Phys. Chem. B 2014, 118, 10085−10091

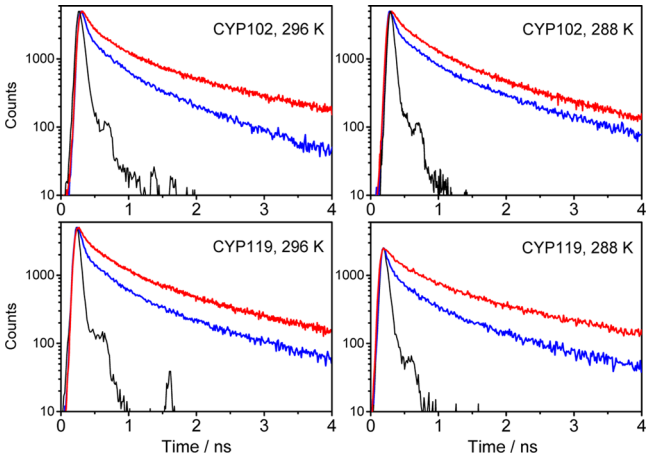

Figure 3. Fluorescence decay of Badan-labeled CYPs. Data for His and Trp mutants are shown in red and blue, respectively.

$$k_q = \frac{1}{\langle \tau_{Trp} \rangle} - \frac{1}{\langle \tau_{His} \rangle} \quad (4)$$

Badan Fluorescence Quenching in Micelles. Addition of a large excess of the surfactant Brij 58 to an aqueous Badan solution (Tris, pH 8) strongly increased Badan solubility and shifted the fluorescence maximum from 550 to 500 nm (Figure S2, Supporting Information), indicating that the micellar environment is a good model for the protein (λ_{em} = 485 nm). Prodan showed very similar behavior. Badan fluorescence decayed single-exponentially, τ_0 = 2.64 ns, whereas Prodan showed a small initial 0.55 ns rise followed by a 3.87 ns decay (all measurements at 550 nm). The lifetime-weighted rise amplitude was less than 10% of the decay amplitude. The rise component is tentatively attributed to a dynamic Stokes shift, whereby the fluorescence intensity initially increases in the red part of the band.[1,2,17,32]

Addition of Trp quenched fluorescence intensity more strongly than the lifetime (Figures 4 and S2, Tables S1 and S2, Supporting Information). This behavior is characteristic of combined dynamic and static quenching,[1,2] which is described by Stern–Volmer (SV) equations (eq 5 and 6).

$$\frac{\tau_0}{\tau} = 1 + k_2\tau_0[\mathrm{Trp}] \quad (5)$$

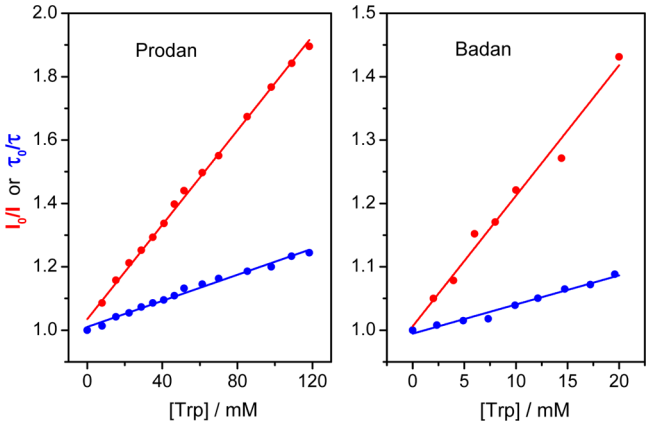

Figure 4. Fluorescence intensity (red) and lifetime (blue) Stern–Volmer plots of Prodan (left) and Badan (right) quenching by tryptophan in Brij 58 micelles. All lifetime values were measured at 550 nm.

$$\frac{I_0}{I} = (1 + k_2\tau_0[\mathrm{Trp}])(1 + K_s[\mathrm{Trp}]) \quad (6)$$

Here, k_2 is the bimolecular rate constant corresponding to dynamic (collisional) quenching and K_s is the stability constant of a supposedly nonemissive Trp–Badan (or Trp–Prodan) complex. (The assumption of an "instantaneous" quenching upon a close contact between the dye and Trp is supported by the lack of any observable ultrafast decay kinetics, indicating that the excited-state lifetime of any such complex is shorter than 50 ps.) Analysis of the lifetime quenching yielded a k_2 value of 1.74×10^9 M^{-1} s^{-1} for Badan and 5.79×10^8 M^{-1} s^{-1} for Prodan (based on τ_{dec} values listed in Table S2, Supporting Information). Lifetime quenching kinetics are virtually independent of the emission wavelength, as was checked for Badan at 500 nm ($k_2 = 1.90 \times 10^9$ M^{-1} s^{-1}) and Prodan at 490 nm (5.74×10^8 M^{-1} s^{-1}). Intensity-based SV plots (Figure 4) yielded (after correction for dynamic quenching) the bimolecular static quenching constant K_s values of 14.7 and 3.5 M^{-1} for Badan and Prodan, respectively. The percentage of the total intensity quenching due to static quenching was estimated as $100K_s/(K_s + k_2\tau_0)$ ~76% for Badan and ~61% for Prodan. Stationary fluorescence spectra also showed a very small blue shift upon Trp addition, from 509 to 504 nm, with an isoemissive point at 484 nm (Figure S3, Supporting

Table 1. Fluorescence Decay Kinetics of Badan-Labeled CYP Mutants

		lifetimes (ns)			τ-weighted amplitudes (%)			amplitudes (%)					
sample	T (K)	τ_1[a]	τ_2	τ_3	B_1	B_2	B_3	A_1	A_2	A_3	average lifetime (ns)[b]	$\langle k_q \rangle$ (s^{-1})	$k_{q,3}$ (s^{-1})
CYP102-Trp	288	0.02[c]	0.48	2.24	33	37	30	96	3	1	0.86	4.5×10^8	1.0×10^8
CYP102-His	288	0.13	0.74	2.92	19	46	35	66	28	6	1.40		
CYP102-Trp	296	0.02[c]	0.40	2.13	32	29	39	96	3	1	0.95	5.1×10^8	1.4×10^8
CYP102-His	296	0.09	0.70	3.03	12	36	52	65	26	9	1.85		
CYP119-Trp	288	0.05	0.50	2.24	30	40	30	87	11	2	0.90	3.7×10^8	7.3×10^7
CYP119-His	288	0.10	0.69	2.68	17	45	38	68	26	6	1.35		
CYP119-Trp	296	0.05	0.53	2.42	31	40	29	88	10	2	0.94	3.8×10^8	8.8×10^7
CYP119-His	296	0.10	0.80	3.07	19	45	35	72	23	5	1.47		

[a]The τ_1 kinetics occur at the limit of the experimental time resolution, and the corresponding lifetime and amplitude values were obtained by IRF deconvolution. Although this might introduce some absolute error, it did not affect significantly the relative change between His- and Trp-containing mutants. [b]Virtually identical average lifetime values were obtained from 4-exponential fits. Accuracy ±50 ps. [c]Estimated, at the limit of IRF deconvolution.

dx.doi.org/10.1021/jp504625d | J. Phys. Chem. B 2014, 118, 10085–10091

Information). This effect indicates the presence of at least two slightly different Badan populations in the micelles, the red-absorbing one being preferentially quenched by Trp.

Electrochemistry. 2-(*N*,*N*-Dimethylamino)naphthalene dyes are known to undergo irreversible electrochemical oxidation that was studied in detail for Prodan.[33] Herein, we report on its reductive electrochemistry that is relevant to the fluorescence quenching by Trp. A cyclic voltammogram (CV) of Prodan in MeCN (Figure 5) showed a nearly reversible

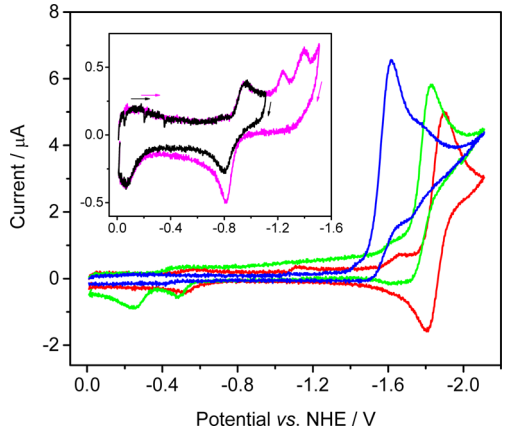

Figure 5. Cyclic voltammetry of Prodan at a Hg electrode (v = 0.5 V/s): red, in acetonitrile (0.1 M Bu_4NPF_6, 0.40 mM Prodan); green, addition of 1% H_2O (0.40 mM Prodan); blue, addition of 17% H_2O (0.44 mM Prodan). Inset: in Britton–Robinson buffer (pH = 7.3).

reduction at $E_{1/2}$ = −1.85 V vs NHE. (The small prewave is due to adsorption of the reduced form.) Changing the solvent from MeCN (ε = 35.9) to a more polar DMSO (ε = 46.5) has only a small effect: the reduction wave stays reversible and shifts to −1.77 V. No reduction is observed in much less polar 1,2-dichloroethane (ε = 10.4) up to −2.2 V. On the other hand, water changes the reduction mechanism and shifts the potential positively: A small addition of water (1%) to the solution of Prodan in MeCN made the reduction chemically irreversible and shifted the cathodic peak potential (E_p^{cat}) by +70 mV while two small anodic peaks appeared at −0.25 and −0.48 V, attributable to reoxidation of the decomposition products of reduced Prodan. CV in MeCN containing 17% H_2O showed a chemically irreversible reduction peak whose E_p^{cat} shifted by +280 mV relative to neat MeCN. The peak shape is consistent with rapid heterogeneous electron transfer, followed by a fast reaction with H_2O (presumably protonation). The CV in H_2O (Britton–Robinson buffer, pH 7.3) showed a quasireversible peak at −0.88 V ($E_p^{an} - E_p^{cat}$ = 0.18 V) followed by two chemically irreversible reduction peaks at −1.24 and −1.40 V. The signal was very weak due to low Prodan solubility. (Results obtained for Prodan should be extendable to Badan because both species contain the same photo- and electroactive group, i.e., 2-(*N*,*N*-dimethylamino)-6-propionylnaphthalene (Figure 1). However, Badan electrochemistry was complicated by the presence of a reducible C–Br bond.)

The excited-state reduction potential of Prodan and Badan in MeCN can be estimated as a sum of the ground-state reduction potential (−1.85 V) and the excited-state energy of 2.5 eV (E_{oo}, estimated from fluorescence spectra), giving the value of +0.6 V vs NHE. Generally, the excited-state redox potential will depend on medium polarity that affects both the ground-state reduction potential and the excited-state energy. However, these two effects could partly compensate each other as decreasing medium polarity increases E_{oo} while shifting the reduction potential negatively. Both dyes become much stronger excited-state oxidants (ca. +1.6 V) in the presence of water, as the reduced form is stabilized by a very rapid reaction with the solvent. The actual value depends on the water accessibility of the dye molecules.

DISCUSSION

Fluorescence lifetimes of the two investigated Badan-labeled CYP-Trp mutants were significantly shorter than those of their His-containing counterparts, indicating that the emissive singlet excited state of Badan is quenched by the proximal Trp residue. To study the Badan–Trp quenching without any possible interfering effects of the protein environment or the heme cofactor, we also investigated Badan (and analogous Prodan) fluorescence quenching by Trp in Brij 58 micelles. Both species concentrate in the micelles, promoting formation of contact pairs. Indeed, we observed very efficient static quenching attributable to the formation of nonemissive $\pi\pi$ complexes between the aromatic Trp-indole groups and Badan (Prodan) inside micelles. These complexes are moderately stable, with association constants of 14.7 M^{-1} (3.5 M^{-1}), and their excited-state lifetimes are much shorter than the instrument time resolution, much less than 50 ps. Residual dynamic quenching, which accounts for 25–40% of the total quenching, is attributable to the highly dynamic nature of the micelles that still allows for diffusive encounters.

Quenching of Badan and Prodan fluorescence can occur by either an energy- or electron-transfer mechanism. Energy transfer can be ruled out, because the population of ^{*1}Trp is energetically uphill (and ^{*3}Trp is slightly uphill and spin-forbidden). The feasibility of an electron-transfer mechanism, i.e., Trp oxidation by excited dyes, can be assessed using electrochemical arguments. Trp is a redox-active amino acid whose indole side chain is oxidized to the corresponding radical cation at rather positive potentials, between +1.02 and +1.21 V vs NHE.[34−37] Above, we have estimated the excited-state reduction potential of Prodan and Badan as +0.6 V in aprotic media and +1.6 V in water. It follows that electron-transfer quenching in aprotic media is endergonic by about 0.5 V (taking $E^{o\prime}(Trp/Trp^{\bullet+})$ = +1.1 V[35]). In CYPs, Badan is located at the protein surface, partly exposed to water (Figure 2). In Brij 58 micelles, the dye and Trp molecules likely occur in the regions between the polyether head groups that are intermixed with water.[38] It is the aqueous solvation that makes the photoreduction of (dimethylamino)naphthalene dyes by Trp thermodynamically possible because water changes the dye reduction mechanism and upshifts the excited-state reduction potential to roughly +1.6 V (the actual value likely depends on the dye exposure to water). Trp oxidation by electronically excited Badan (Prodan) in the present systems is thus thermodynamically favorable by ≤0.5 V and ET is coupled to a very fast reaction between the solvating water molecules to the reduced dye (presumably proton transfer).

Having established Badan photoreduction by Trp as the most likely quenching mechanism, we turn our attention to the fluorescence decay kinetics of Badan-labeled CYPs. Both CYP102-His and CYP119-His exhibited multiexponential behavior that probably reflects conformational heterogeneity, together with medium relaxation dynamics[39] in the Badan vicinity. The longest lifetime measured for the His-containing mutants (τ_3, ∼3 ns) is longer than that observed in aqueous

dx.doi.org/10.1021/jp504625d | *J. Phys. Chem. B* 2014, 118, 10085−10091

solutions (1.3−1.4 ns, Prodan)[40] or in Brij micelles (2.64 ns, Table S1, Supporting Information), indicating that the Badan label is to some extent shielded from the solvent and oriented to disfavor energy transfer to the heme. The two faster components likely arise from conformations where Badan is more exposed and/or quenched by Förster energy transfer to the heme. (Indeed, heme cofactors are known to quench fluorescence of (dimethylamino)naphthalene dyes, such as Dansyl.[6]) Crystal structures of unlabeled CYP102-Trp (pdb 2IJ2) and CYP102-His (to be published) show that the five-membered part of the Trp96 indole ring of CYP102-Trp overlaps perfectly with the imidazole ring of the His mutant. The distances and orientations of the heme also are comparable. In both mutants, the Badan-bearing Cys97 is, on average, 6 Å away from the aromatic side chain (His96 or Trp96). The structure also reveals the presence of various rotamers that introduces significant variability in positions and orientations of the Cys97 sulfur atom and, hence, of the attached Badan label. The similarity between the structures of the Trp- and His-containing mutants supports our conclusion that the fluorescence lifetime decrease on going from CYP102-His to CYP102-Trp is attributable solely to the photoinduced ET between excited Badan and Trp. (Presumably, this conclusion remains valid also for CYP119, where only the structure of the His mutant is available, pdb 1IO7.) In particular, replacing the His residue proximal to Badan by Trp caused partial fluorescence quenching, with an average quenching rate constant of about 4×10^8 M^{-1} s^{-1} for both CYP102-Trp and CYP119-Trp (at 288 K). Quenching influences all three fluorescence decay components (Table 1). The most pronounced change was observed for the shortest, tens-of-picoseconds, component that became much shorter lived and whose relative amplitude strongly increased. This fastest quenching process presumably occurs in a protein conformation where the Trp-indole and Badan make a close contact, resulting in almost complete quenching. The amplitude increase then reflects a change in conformational distribution, whereby close Trp−Badan contact formation is driven by $\pi\pi$ and/or hydrophobic interactions. Quenching of the longest lifetime τ_3 ($k_{q,3} = 1 \times 10^8$ and 7×10^7 s^{-1} for CYP102 and CYP119, respectively) is too slow for a contact pair. Instead, it probably corresponds to long-range ET from Trp to the excited Badan label.

We conclude that (dimethylamino)naphthalene-based dyes Badan and Prodan can behave as photooxidants whose excited-state reduction potentials vary from about +0.6 V (vs NHE) in polar aprotic media (MeCN) to approximately +1.6 V in water, where reduction is presumably coupled to proton transfer. Fluorescence of these (dimethylamino)naphthalene dyes is quenched by close-lying tryptophan in proteins as well as micelles. Excited-state ET reactions in Badan-labeled CYPs occur in several kinetics steps whose lifetimes range from tens of picoseconds to about 10 ns, presumably depending on protein conformation as well as the relative orientation of the Badan and indole aromatic groups. The possibility of photoinduced ET must be considered whenever (dimethylamino)naphthalene dyes are used as fluorescence protein labels, as this reaction channel can complicate the interpretation of FRET experiments as well as analyses of solvation dynamics studied by time-resolved fluorescence spectroscopy. On the other hand, as nanosecond Badan fluorescence quenching kinetics are expected to be sensitive to structural and conformational factors, Badan protein labeling could be employed to investigate short-range (≤10 Å) intraprotein interactions and conformational changes due to folding or substrate binding.

■ ASSOCIATED CONTENT

Ⓢ Supporting Information

Stationary fluorescence spectra of the Badan-labeled CYPs and Badan-containing micelles, area-normalized Badan fluorescence spectra in micelles at different Trp concentrations, tables of Trp concentration dependence of Badan and Prodan fluorescence lifetimes in micelles. This material is available free of charge via the Internet at http://pubs.acs.org.

■ AUTHOR INFORMATION

Corresponding Authors

*H. B. Gray. E-mail: hbgray@caltech.edu.
*A. Vlček. E-mail: a.vlcek@qmul.ac.uk.
*M. Hof. E-mail: martin.hof@jh-inst.cas.cz.

Notes

The authors declare no competing financial interest.

■ ACKNOWLEDGMENTS

This research was supported by the Grant Agency of the Czech Republic (P106/12/G016) and the Ministry of Education of the Czech Republic program Kontakt II (grant LH13015). M.H. acknowledges financial support by ASCR via the Praemium Academiae award. Work at Caltech was supported by NIH grant DK019038 to H.B.G. and a Summer Undergraduate Research Fellowship (SURF) to K.E.L.

■ REFERENCES

(1) Lakowicz, J. R. *Principles of Fluorescence Spectroscopy*, 3rd ed.; Springer: New York, 2006.
(2) Valeur, B. *Molecular Fluorescence. Principles and Applications*; Wiley-VCH: Weinheim, 2002.
(3) Doose, S.; Neuweiler, H.; Sauer, M. Fluorescence Quenching by Photoinduced Electron Transfer: A Reporter for Conformational Dynamics of Macromolecules. *ChemPhysChem* **2009**, *10*, 1389−1398.
(4) Doose, S.; Neuweiler, H.; Sauer, M.; Close, A. Look at Fluorescence Quenching of Organic Dyes by Tryptophan. *ChemPhysChem* **2005**, *6*, 2277−2285.
(5) Tsalkova, T. N.; Davydova, N. Y.; Halpert, J. R.; Davydov, D. R. Mechanism of Interactions of R-Naphthoflavone with Cytochrome P450 3A4 Explored with an Engineered Enzyme Bearing a Fluorescent Probe. *Biochemistry* **2007**, *46*, 106−119.
(6) Dunn, A. R.; Hays, A.-M. A.; Goodin, D. B.; Stout, C. D.; Chiu, R.; Winkler, J. R.; Gray, H. B. Fluorescent Probes for Cytochrome P450 Structural Characterization and Inhibitor Screening. *J. Am. Chem. Soc.* **2002**, *124*, 10254−10255.
(7) Holt, A.; Koehorst, R. B. M.; Rutters-Meijneke, T.; Gelb, M. H.; Rijkers, D. T. S.; Hemminga, M. A.; Killian, J. A. Tilt and Rotation Angles of a Transmembrane Model Peptide as Studied by Fluorescence Spectroscopy. *Biophys. J.* **2009**, *97*, 2258−2266.
(8) Gray, H. B.; Winkler, J. R. Long-Range Electron Transfer. *Proc. Natl. Acad. Sci. U. S. A.* **2005**, *102*, 3534−3539.
(9) Vaiana, A. C.; Neuweiler, H.; Schulz, A.; Wolfrum, J.; Sauer, M.; Smith, J. C. Fluorescence Quenching of Dyes by Tryptophan: Interactions at Atomic Detail from Combination of Experiment and Computer Simulation. *J. Am. Chem. Soc.* **2003**, *125*, 14564−14572.
(10) Neuweiler, H.; Johnson, C. M.; Fersht, A. R. Direct Observation of Ultrafast Folding and Denatured State Dynamics in Single Protein Molecules. *Proc. Natl. Acad. Sci. U. S. A.* **2009**, *106*, 18569−18574.
(11) Neuweiler, H.; Banachewicz, W.; Fersht, A. R. Kinetics of Chain Motions Within a Protein-Folding Intermediate. *Proc. Natl. Acad. Sci. U. S. A.* **2010**, *107*, 22106−22110.

(12) Goldberg, J. M.; Batjargal, S.; Chen, B. S.; Petersson, E. J. Thioamide Quenching of Fluorescent Probes through Photoinduced Electron Transfer: Mechanistic Studies and Applications. *J. Am. Chem. Soc.* **2013**, *135*, 18651−18658.
(13) Sancar, A. Structure and Function of DNA Photolyase and Cryptochrome Blue-Light Photoreceptors. *Chem. Rev.* **2003**, *103*, 2203−2237.
(14) Tanaka, F.; Chosrowjan, H.; Taniguchi, S.; Mataga, N.; Sato, K.; Nishina, Y.; Kiyoshi Shiga, K. Donor-Acceptor Distance-Dependence of Photoinduced Electron-Transfer Rate in Flavoproteins. *J. Phys. Chem. B* **2007**, *111*, 5694−5699.
(15) Byrdin, M.; Lukacs, A.; Thiagarajan, V.; Eker, A. P. M.; Brettel, K.; Vos, M. H. Quantum Yield Measurements of Short-Lived Photoactivation Intermediates in DNA Photolyase: Toward a Detailed Understanding of the Triple Tryptophan Electron Transfer Chain. *J. Phys. Chem. A* **2010**, *114*, 3207−3214.
(16) Lukacs, A.; Eker, A. P. M.; Byrdin, M.; Brettel, K.; Vos, M. H. Electron Hopping through the 15 Å Triple Tryptophan Molecular Wire in DNA Photolyase Occurs within 30 ps. *J. Am. Chem. Soc.* **2008**, *130*, 14394−14395.
(17) Jurkiewicz, P.; Sýkora, J.; Olžinska, A.; Humpolíčková, J.; Hof, M. Solvent Relaxation in Phospholipid Bilayers: Principles and Recent Applications. *J. Fluoresc.* **2005**, *15*, 883−894.
(18) Klymchenko, A. S.; Mely, Y. Fluorescent Environment-Sensitive Dyes as Reporters of Biomolecular Interactions. *Prog. Mol. Biol. Transl. Sci.* **2013**, *113*, 35−58.
(19) Novaira, M.; Biasutti, M. A.; Silber, J. J.; Correa, N. M. New Insights on the Photophysical Behavior of PRODAN in Anionic and Cationic Reverse Micelles: From Which State or States Does It Emit? *J. Phys. Chem. B* **2007**, *111*, 748−759.
(20) Guha, S.; Sahu, K.; Roy, D.; Mondal, S. K.; Roy, S.; Bhattacharyya, K. Slow Solvation Dynamics at the Active Site of an Enzyme: Implications for Catalysis. *Biochemistry* **2005**, *44*, 8940−8947.
(21) Samaddar, S.; Mandal, A. K.; Mondal, S. K.; Sahu, K.; Bhattacharyya, K.; Roy, S. Solvation Dynamics of a Protein in the Pre Molten Globule State. *J. Phys. Chem. B* **2006**, *110*, 21210−21215.
(22) Saxla, T.; Khana, F.; Matthews, D. R.; Zhia, Z.-L.; Rolinski, O.; Ameer-Beg, S.; Pickup, J. Fluorescence Lifetime Spectroscopy and Imaging of Nano-Engineered Glucose Sensor Microcapsules Based on Glucose/Galactose-Binding Protein. *Biosens. Bioelectron.* **2009**, *24*, 3229−3234.
(23) Batabyal, S.; Mondol, T.; Pal, S. K. Picosecond-Resolved Solvent Reorganization and Energy Transfer in Biological and Model Cavities. *Biochimie* **2013**, *95*, 1127−1135.
(24) Bouley Ford, N. D.; Dong-Woo Shin, D.-W.; Gray, H. B.; Winkler, J. R. Intrachain Contact Dynamics in Unfolded Cytochrome cb_{562}. *J. Phys. Chem. B* **2013**, *117*, 13206−13211.
(25) Yamada, S.; Bouley Ford, N. D.; Keller, G. E.; Ford, W. C.; Gray, H. B.; Winkler, J. R. Snapshots of a Protein Folding Intermediate. *Proc. Natl. Acad. Sci. U. S. A.* **2013**, *110*, 1606−1610.
(26) Mondol, T.; Batabyal, S.; Pal, S. K. Ultrafast Electron Transfer in the Recognition of Different DNA Sequences by a DNA-Binding Protein with Different Dynamical Conformations. *J. Biomol. Struct. Dyn.* **2012**, *30*, 362−370.
(27) Girvan, H. M.; Seward, H. E.; Toogood, H. S.; Cheesman, M. R.; Leys, D.; Munro, A. W. Structural and Spectroscopic Characterization of P450 BM3Mutants with Unprecedented P450 Heme Iron Ligand Sets. *J. Biol. Chem.* **2007**, *282*, 564−572.
(28) Kishan, K. V. R.; Newcomer, M. E.; Rhodes, T. H.; Guilliot, S. D. Effect of pH and Salt Bridges on Structural Assembly: Molecular Structures of the Monomer and Intertwined Dimer of the Eps8 SH3 Domain. *Protein Sci.* **2001**, *10*, 1046−1055.
(29) Ener, M. E.; Lee, Y.-T.; Winkler, J. R.; Gray, H. B.; Cheruzel, L. Photooxidation of Cytochrome P450-BM3. *Proc. Natl. Acad. Sci. U. S. A.* **2010**, *107*, 18783−18786.
(30) Klammt, C.; Schwarz, D.; Fendler, K.; Haase, W.; Dotsch, V.; Bernhard, F. Evaluation of Detergents for the Soluble Expression of Alpha-Helical and Beta-Barrel-Type Integral Membrane Proteins by a Preparative Scale Individual Cell-Free Expression System. *FEBS J.* **2005**, *272*, 6024−6038.
(31) Pavlishchuk, V. V.; Addison, A. W. Conversion Constants for Redox Potentials Measured Versus Different Reference Electrodes in Acetonitrile Solutions at 25°C. *Inorg. Chim. Acta* **2000**, *298*, 97−102.
(32) Horng, M. L.; Gardecki, J. A.; Papazyan, A.; Maroncelli, M. Subpicosecond Measurements of Polar Solvation Dynamics: Coumarin 153 Revisited. *J. Phys. Chem.* **1995**, *99*, 17311−17337.
(33) Moressi, M. B.; Zón, M. A.; Fernández, H. Electrochemical Oxidation of 6-propionyl-2-(N,N-dimethylamino)naphthalene (Prodan) in Acetonitrile on Pt Electrodes: Reversible Dimerization of Prodan Radical Cations. *Can. J. Chem.* **2002**, *80*, 1232−1241.
(34) Harriman, A. Further comments on the Redox Potentials of Tryptophan and Tyrosine. *J. Phys. Chem.* **1987**, *91*, 6102−6104.
(35) Gagliardi, C. J.; Binstead, R. A.; Thorp, H. H.; Meyer, T. J. Concerted Electron Proton Transfer (EPT) in the Oxidation of Tryptophan with Hydroxide as a Base. *J. Am. Chem. Soc.* **2011**, *133*, 19594−19597.
(36) Tommos, C.; Skalicky, J. J.; Pilloud, D. L.; Wand, A. J.; Dutton, P. L. De Novo Proteins as Models of Radical Enzymes. *Biochemistry* **1999**, *38*, 9495−9507.
(37) Stewart, D. J.; Napolitano, M. J.; Bakhmutova-Albert, E. V.; Margerum, D. W. Kinetics and Mechanisms of Chlorine Dioxide Oxidation of Tryptophan. *Inorg. Chem.* **2008**, *47*, 1639−1647.
(38) Schefer, J.; McDaniel, R.; Schoenborn, B. P. Small-Angle Neutron Scattering Studies on Brij-58 Micelles. *J. Phys. Chem.* **1988**, *92*, 729−732.
(39) Jesenská, A.; Sýkora, J.; Olzynska, A.; Brezovský, J.; Zdráhal, Z.; Damborský, J.; Hof, M. Nanosecond Time-Dependent Stokes Shift at the Tunnel Mouth of Haloalkane Dehalogenases. *J. Am. Chem. Soc.* **2009**, *131*, 494−501.
(40) Sengupta, B.; Guharay, J.; Sengupta, P. K. Characterization of the Fluorescence Emission Properties of Prodan in Different Reverse Micellar Environments. *Spectrochim. Acta, Part A* **2000**, *56*, 1433−1441.